Scanning Microscopy

Volume 1 | Number 3 Article 51

5-6-1987

Myogenesis in vitro as Seen with the Scanning Electron Microscope

Y. Shimada
Chiba University

M. Komiyama
Chiba University

M. Shiozaki
Chiba University

Y. Isobe
Chiba University

S. Masuko
Chiba University

Scanning Microscopy, Vol. 1, No. 3, 1987 (Pages 1377-1386) 0891-7035/87$3.00+.00
Scanning Microscopy International, Chicago (AMF O'Hare), IL 60666 USA

MYOGENESIS IN VITRO AS SEEN WITH THE SCANNING ELECTRON MICROSCOPE

Y. Shimada[1,2*], M. Komiyama[1,3], M. Shiozaki[1], Y. Isobe[1,4] and S. Masuko[1,5]

[1]Department of Anatomy, School of Medicine, Chiba University, Chiba 280
[2]Department of Physiological Genetics, National Institute of Genetics, Mishima 411
[3]Department of Anatomy, Faculty of Physical Education, The International Budo University, Katsuura 299-52
[4]Department of Anatomy and Cell Biology, State University of New York, Health Science Center, Syracuse, N.Y. 13210
[5]Department of Anatomy, Saga Medical School, Saga 840-01

(Received for publication February 23, 1987, and in revised form May 06, 1987)

Abstract

In this paper, we review our recent observations by scanning electron microscopy (SEM) on the differentiation of the cell surface and cytoplasmic organelles in embryonic chick skeletal muscle cells in vitro. The changes of the surface structures of myoblasts during mitosis were essentially similar to those of other cell types, but the characteristic spindle shape of myoblasts did not change throughout most of this period. Cytoskeletal structures under the sarcolemma were examined by Triton extraction and metal coating. Cells in S, G_2 and M possessed a dense, and those in G_1 a loose filament network under the membrane. Myotubes possessed a dense network under the sarcolemma. In the fusion area between a myoblast and a myotube, the cytoskeletal domain of the former could be distinguished from the latter because of the mosaic appearance of the subsarcolemmal cytoskeletal network. This network was composed predominantly of 10-13 nm filaments; they were identified as actin filaments because of their decoration with myosin subfragment-1. Triton treatment and thiocarbohydrazide-osmium staining allowed us to visualize myofibrils. They ran in the direction of inferred stress lines brought about by elongation and adhesion of the cells to substrate. Intracellular membranous organelles could be seen by the freeze-polishing and osmium-maceration procedure. Mitochondria exhibited complex irregular branchings. T system tubules ran a tortuous course. Sarcoplasmic reticula with occasional dilatations were connected to each other. The results are of sufficient promise to encourage more extensive analysis of myogenesis by SEM.

KEY WORDS: Myogenesis, cell cycle, cell surface, cytoskeleton, stress fibers, myofibrillogenesis, mitochondria, T tubule, sarcoplasmic reticulum.

*Address for correspondence:
Yutaka Shimada
Department of Anatomy
School of Medicine, Chiba University
Chiba 280, Japan Phone No. (0472) 22-7171

Introduction

During muscle development, many changes take place in the structural, biochemical and functional properties of cells. With the advent of transmission electron microscopy (TEM), fine structural aspects of these cells have been studied extensively and many problems in this field have been solved (6, 7, 8, 26, 29, 30). However, to obtain a three-dimensional perspective of the organization of cell surfaces and intracellular organelles of these cells with TEM, tedious and inconvenient serial sectioning and reconstruction must be carried out. This limitation has been overcome by using high voltage TEM of whole mount cells (21, 22). However, this method also has obstacles. Whole mount TEM provides images in which many structures are superimposed, making interpretation difficult; there still exists considerable controversy about the validity of some of the structures visualized in samples prepared by high voltage TEM (24).

We have been examining the ultrastructural differentiation of myogenic cells by scanning electron microscopy (SEM) (12, 15, 18, 19, 27). This technique minimizes the sampling problem presented by TEM and, in combination with suitable specimen preparation methods, it permitted detailed three-dimensional analyses of phenomena occurring at the surface as well as within the cell. In this paper we review our recent SEM observations on the development of cell surface, cytoskeletons, myofibrils and cytoplasmic membranous organelles in skeletal muscle cells in vitro.

Materials and Methods

Muscle Cell Cultures

Primary embryonic skeletal muscle cell cultures were prepared from 11-day-old chick pectoral muscles according to the method of Shimada et al. (30). Cell suspensions, enriched in myogenic cells by a differential adhesion procedure (33), were used for the present experiment. The cultures were maintained on glass coverslips placed on the bottom of plastic culture dishes. These coverslips were precoated with evaporated carbon, sputter-coated with gold-palladium, and finally overlaid with gelatin.

The culture medium consisted of Eagle's minimal essential medium with glutamine, 15% horse serum, 5% embryo extract, and penicillin-streptomycin in concentrations of 50 U and 50 µg/ml, respectively. Cultures were kept at 37°C in an atmosphere of 5% CO_2 in air at saturation humidity.

Thymidine Block

Synchronized populations of myoblasts were obtained by the thymidine block method (9). Mitotic populations on cover glasses in cultures were exposed to 5 mM thymidine for 10-12 h after plating. This was sufficient time for many of the cells to complete the G_1 period, since the total generation time of 2 day cultures is 10 h, and it is shorter in younger cultures (1). The cells which are in the S phase at the beginning of the treatment remain in the S phase. Therefore, from the thymidine treated cultures, mixed populations of cells at late G_1 and S periods can be obtained.

The blocked cells were released by removal of the thymidine with a change of the medium. Since the S period of these cells is about 5 h, G_2 is 1.5 h, M 0.5-1 h, and G_1 is 3-12 h (the younger the culture, the shorter the duration of G_1) (1, 20), samples were fixed at 6 and 8 h after release of the block to provide cells in late G_2 and M. By phase contrast microscopy, cells in the M phase could also be identified by the separation of two daughter chromosomes and by a cytoplasmic constriction. Cells in early G_1 were obtained 1 h after observation of mitosis.

Scanning Electron Microscopy

Specimens for SEM were prepared by the following procedures: (1) For observation of the surface structure of cells grown on coverslips, the materials were fixed in 2.5% glutaraldehyde in 0.1 M cacodylate buffer at pH 7.2 for 2 h and postfixed in OsO_4 in the same buffer for 1 h. They were then electroconductively stained with thiocarbohydrazide and osmium (TCH-OsO_4) (16). Samples were dehydrated with ethanol and amyl acetate, and critical-point dried from liquid CO_2. (2) To observe cytoskeletal structures under the cell membrane, the samples were treated with 0.5% Triton X-100 (Triton) in potassium buffer (70 mM KCl, 5 mM $MgCl_2$, 3 mM EGTA, 30 mM HEPES and 0.1 mM phenylmethylsulfonyl fluoride, pH 7.0) at room temperature for 3 min, and fixed with 2.5% glutaraldehyde in the same buffer for 60 min. They were then treated with 0.2% tannic acid for 30 min and finally with 1% OsO_4 for 60 min. After dehydration and critical-point drying, the materials were coated with gold-palladium (thickness: 2-4 nm) in a sputter-coater (Emscope SC500A). For myosin subfragment-1 (S-1) decoration of actin-containing structures, Triton-extracted cells were treated with S-1 at a concentration of 1 mg/ml in potassium buffer before the fixation step. (3) For the observation of developing myofibrils within cells, the cultures were incubated in 0.5% Triton in KMP buffer (50 mM KCl, 5 mM $MgCl_2$, 2 mM EGTA, and 10 mM K-phosphate buffer, pH 7.5) at 37°C for 10-30 min. They were immersed in 2% glutaraldehyde in KMP buffer for 30 min, postfixed in 1% OsO_4 in the same buffer for 30 min, and finally stained with the TCH-OsO_4 method. The TCH-OsO_4 cycle was repeated once more, and the samples were dehydrated in ethanol and amyl acetate and dried by CO_2 critical-point drying. (4) Some other samples were prepared for observing intracellular membranous structures according to the method of Inoué and Osatake (11). Cultures were fixed in 1% OsO_4 in 0.1 M cacodylate buffer at pH 7.2 for 1 h, and transferred to 25% and 50% dimethyl sulfoxide (DMSO) solutions for 30 min each. They were then frozen in liquid nitrogen and abraded with a film covered with fine particles of aluminum oxide (Imperial Lapping Film, 3M Co.). Each specimen was abraded with a series of successively finer film (grain sizes: 3, 1, and 0.3 µm) on a liquid-nitrogen chilled aluminum plate. The samples were thawed by immersing into 50% DMSO, and post-fixed in 1% OsO_4 for 1 h. They were subsequently treated with 0.1% OsO_4 for 2-3 days at 20°C to remove excessive cytoplasmic matrix. After conductive staining with 2% tannic acid and 1% OsO_4, they were dehydrated and critical-point dried. The dried samples were sputter-coated with gold-palladium (thickness: 2-4 nm).

All specimens with and without metal-coating were examined with a scanning electron microscope (Hitachi HFS-2S or ISI DS-130) operated at 15-25 kV.

Surface Morphology

Cells treated with thymidine were spindle-shaped with bipolar tapering cytoplasmic extensions which possessed filopodia, usually together with ruffling extended onto the substrate from the tip. These cells were smooth on their surface and almost devoid of microvilli (Fig. 1a). Although, within this cell population, cells in the late G_1 and S phases were known to be present, two kinds of cells could not be identified depending upon different shapes and surface morphologies.

Cells fixed 6 h after the release had become bulged at their perinuclear region. The bipolar cytoplasmic extensions had become shorter. From the tip of these extensions, some long slender filopodia usually extended to the substrate. On the surface of these cells, microvilli began to appear and some blebs were present (Fig. 1b). Since these cells possessed the surface characteristics of both stages G_2 and M of other cell types (23), they were concluded to be premitotic cells in the late G_2 phase.

8 h after the release, many cells had become rounded (Figs. 1c-e). Spherical cells with numerous microvilli appeared to be in prophase or metaphase (Fig. 1c), and elliptical cells with a constriction in anaphase (Fig. 1d). Long microvilli from both sides of the longitudinal axis of the oblong spheroid cell became extended and attached to the substrate. Rounded cells in pair-association appeared to be cells in telophase (Fig. 1e). They possessed filopodia at their base which appeared to have held the cells to the substrate during mitosis and cytokinesis. Microvilli had decreased in number from the cells in anaphase.

Cells fixed about 1 h after cell division

(in early G_1) were still in pairs with the adjacent edges representing the plane of earlier cleavage. By this stage the cells had lost their spherical form, and the adjacent edges of each cell were extended and tapered. These cells had only a few microvilli and blebs and, thus, possessed a relatively smooth surface. Ruffling was a characteristic feature of these cells but it was confined to the tips of the bipolar extensions not in contact with other cells (Fig. 1f).

These observations on the changes in surface structure that occur in association with the cell cycle are essentially similar to those reported earlier in Chinese hamster ovary (CHO) cells (23) and BHK cells (5). Thus, the changes in surface structure observed here are the general occurrences related to mitosis. However, cells of each type retain their characteristic shape throughout most of the mitotic period (in the case of myoblasts, the spindle shape).

A single treatment with thymidine may not be sufficient to obtain optimal synchronization of myoblasts in culture, because cells which are in the S phase at the moment of the beginning of the treatment will not be synchronized (9), and there are some varieties in the length of each mitotic phase in populations of cultured myoblasts (1). The ^3H- and ^{14}C-thymidine double-labeling autoradiography (32) enabled us to distinguish myoblasts in the S and G_2 phases. By SEM combined with this double-labeling method, we have reported previously the surface morphology of myoblasts in these specified points of the cell cycle (18). The cells presented in Figs. 1a and 1b were from cultures enriched in cells in the S (or G_1) and G_2 phases, respectively, and show similar surface structures to those in each phase reported previously (18). Light microscopy was used to choose cells in M from cultures enriched in cells in the M phase. Cells in early G_1 were selected from cultures enriched in cells in early G_1. Thus, we are confident that cells presented in Fig. 1 are true representatives of each phase of mitosis.

Cytoskeleton

By SEM of Triton-extracted, critical point-dried and metal-coated muscle cells grown on cover glasses, we examined the overall subsarcolemmal cytoskeletons during the cell cycle and fusion.

Under the sarcolemma of cells in the S phase, an intricate cytoskeletal filament network was seen (Fig. 2a). Within this network, densely packed filament bundles were discernible, running along the long axis of slender cells (Fig. 2b). In cells in G_2, a dense and highly interconnected filament network was seen, and it appeared as a sheath enveloping all the cells (Fig. 3a). Lon-

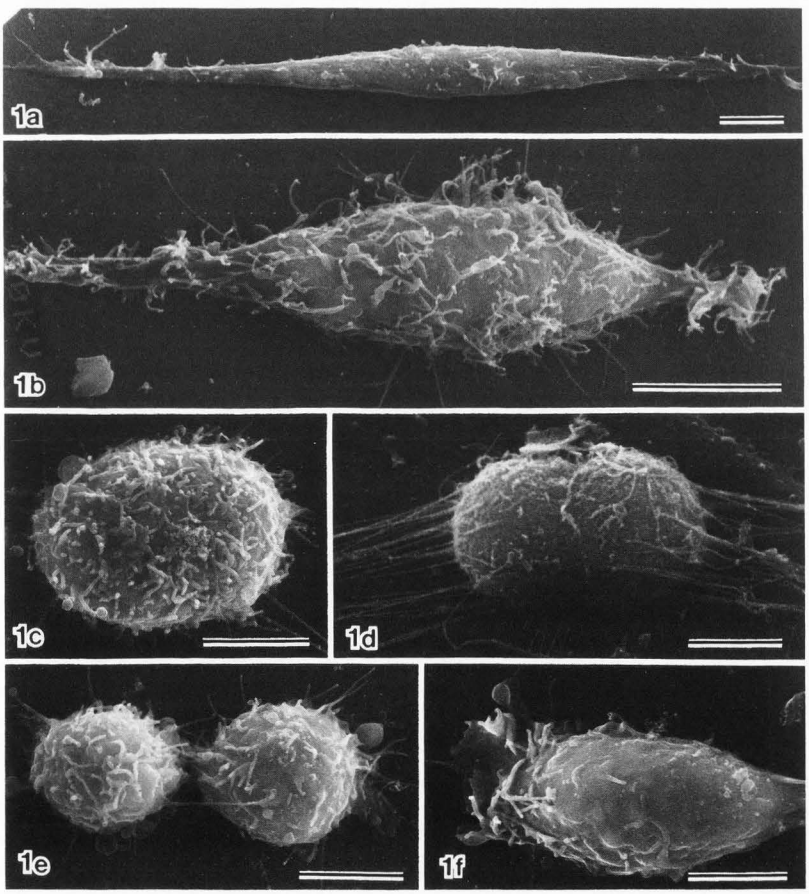

Fig. 1. Changes of the surface structure of myogenic cells in vitro during mitosis. (a) Cells in the late G_1 or S phase are spindle-shaped with a few short microvilli and have a smooth surface. (b) Cells in the late G_2 have shorter bipolar cytoplasmic extensions and are bulged at their perinuclear region. These cells begin to possess microvilli and some blebs. (c) Cells in prophase or metaphase are rounded and possess many microvilli. (d) Elliptical cells with a constriction appear to be cells in anaphase. Long microvilli extend from opposite ends of the cell and attach to the substrate. (e) Rounded cells associated in pairs are cells in telophase. They have fewer microvilli and possess filopodia at their base. (f) In the early G_1 phase, cells are elongated. Their surface becomes smooth. Ruffling is observed at the tip of a cell not in contact with the other cell in a pair. Bar = 5 μm.

gitudinally arranged filament bundles were no longer apparent in this network of spindle-shaped cells (Fig. 3b). At the M phase, rounded cells still possessed a dense and complex cytoskeletal network under the cell membrane (Figs. 4a, b).

In contrast, fusiform cells in the G_1 phase, which probably left the proliferative cycle and prepared for fusion, had a loose cytoskeletal network under the sarcolemma (Fig. 5a). This loose network was formed by complex anastomotic webs of filaments extending just beneath the extracted cell membranes (Fig. 5b).

Myotubes in vitro again began to possess a dense and intricate cytoskeletal network under the sarcolemma. Within this network, bundles of filaments were again seen running along the length of the myotubes (Figs. 6a, b). This subsarcolemmal cytoskeletal network of myotubes somewhat resembles that of myoblasts in the S phase.

In the area where a myoblast, presumably in the late G_1 phase, closely apposed a myotube, the cytoskeletal network of the former cell was attached to and continuous with that of the latter. However, the cytoskeletal domain belonging to the myoblast was distinguishable from that of the myotube because of the difference in their densities (Fig. 6b). This result suggests that the admixture of the contents of two cells after cytoplasmic fusion was poor. This observation is in accord with our previous findings by thin section TEM that the diffusion of myoblast con-

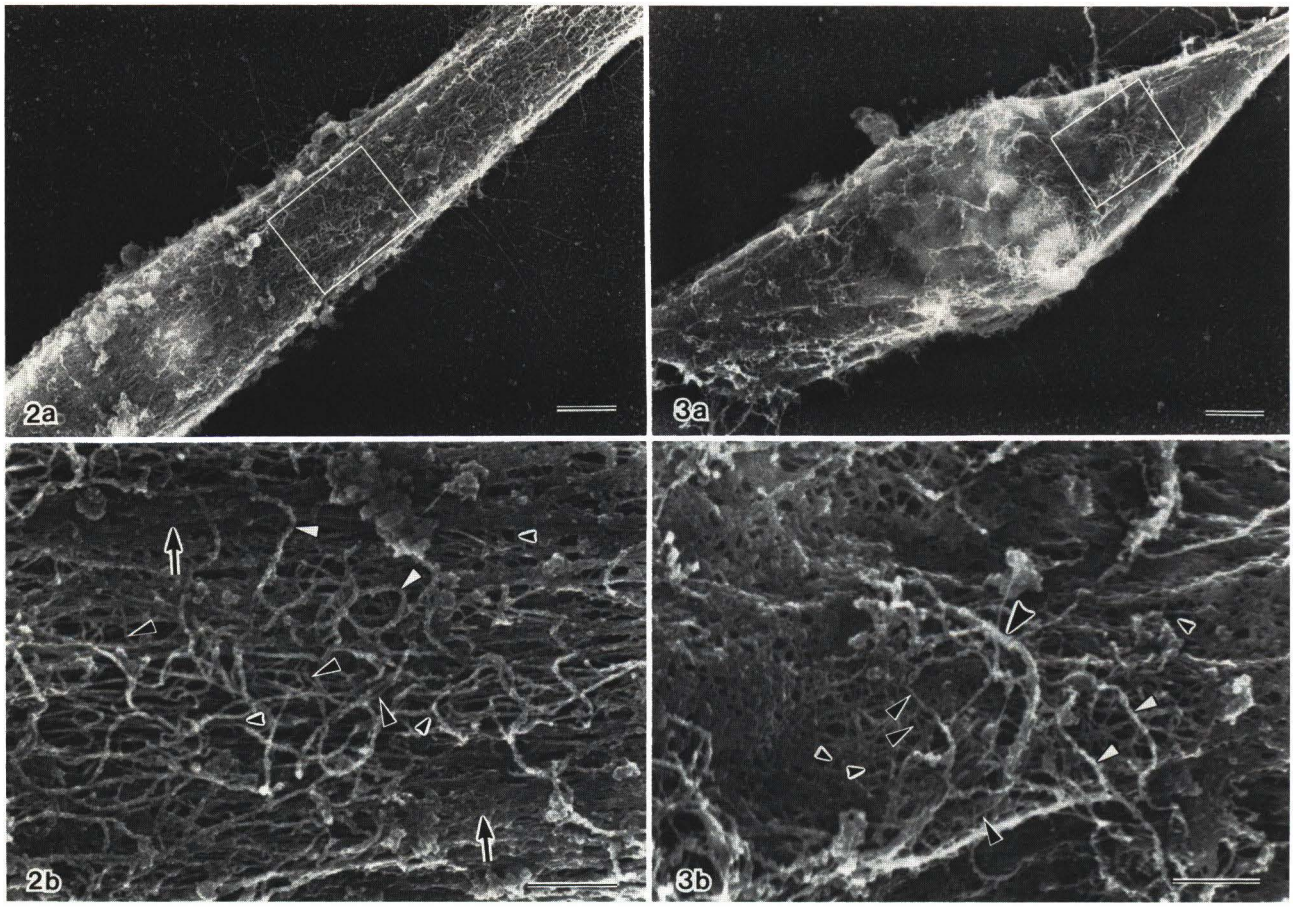

Figs. 2-6. Subsarcolemmal cytoskeletons visualized by treatment of cells with Triton and light coating with metal. Cells in the S (Fig. 2), G_2 (Fig. 3) and M phases (Fig. 4) possess a dense and highly interconnected cytoskeletal filament network under the cell membrane. Cells in the G_1 phase (Fig. 5) have a loose network under the sarcolemma. In Fig. 6, a myoblast (MB) recently fused with a myotube (MT) can be seen. As myotubes mature, they begin to have a dense network under the plasmalemma. These subsarcolemmal networks consist of filaments measuring 10-13 (medium-sized black arrowheads) and 15-18 nm (medium-sized white arrowheads) in diameter after metal-coating. Stress fibers are seen within this network (arrows). Short filaments of less than 8 nm in diameter (small black arrowheads) cross-connect the lateral surfaces of other filaments with each other. Cytoskeletons in demembraned microvilli measure about 100 nm (large arrowheads in Fig. 3b). (a) Bar = 2 μm; (b) Higher magnification view of the rectangles in (a). Bar = 0.5 μm.

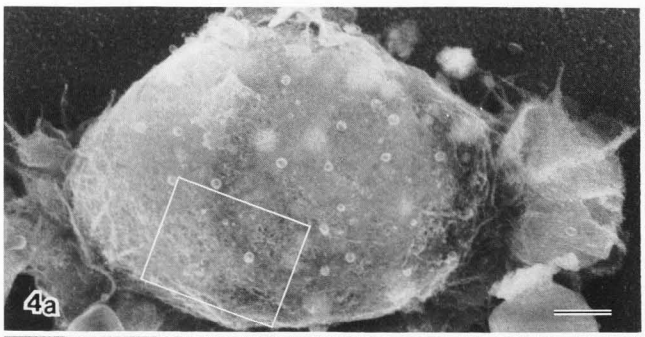

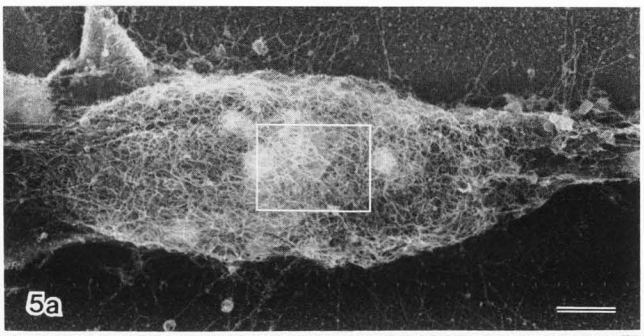

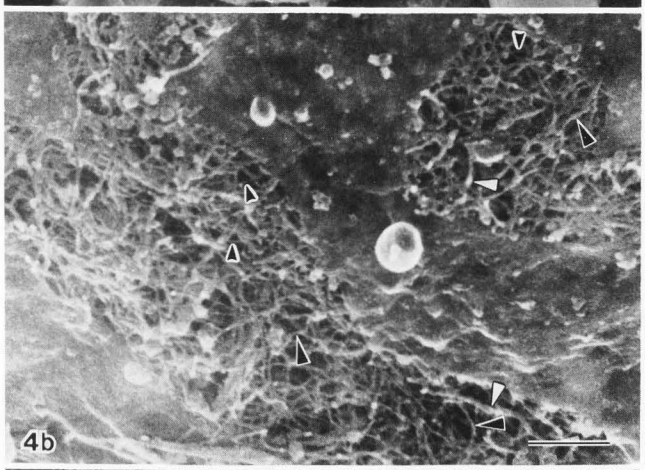

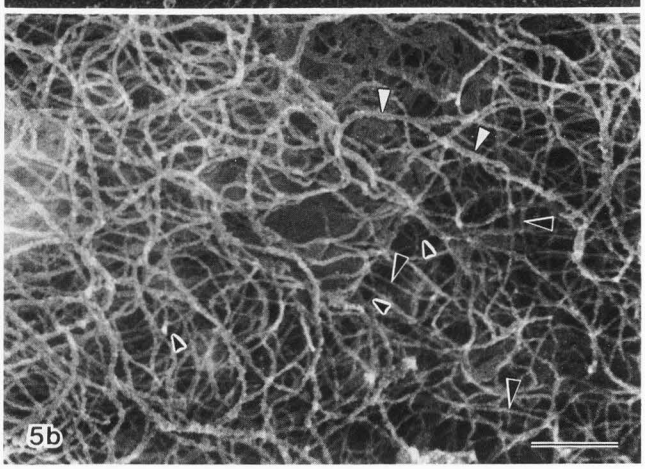

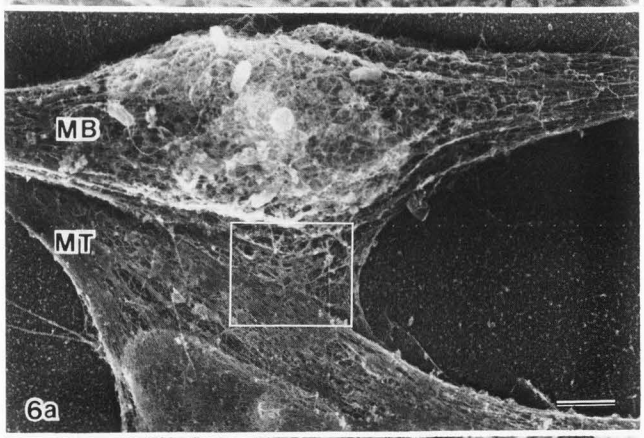

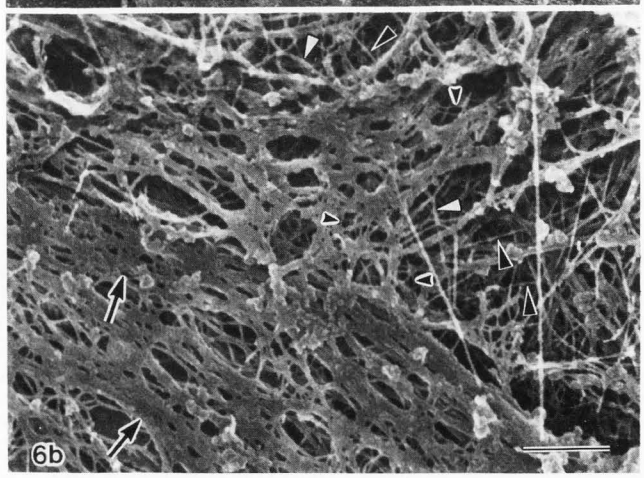

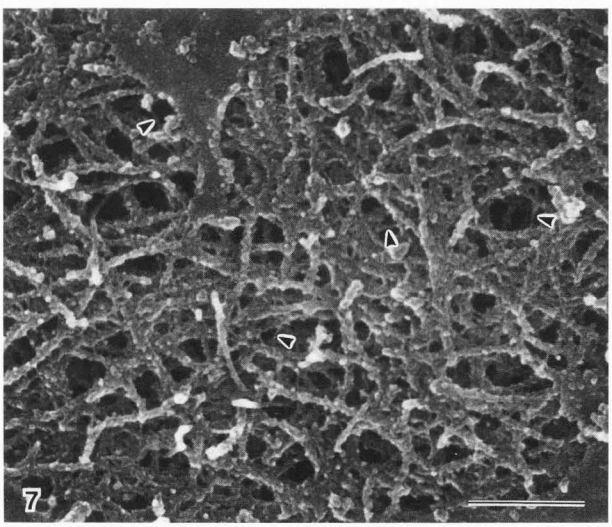

Fig. 7. Subsarcolemmal cytoskeletons treated with Triton and S-1. Filaments of 10-13 nm were thickened and studded with numerous globular structures. Short filaments of less than 8 nm (small black arrowheads) are observed to cross-connect the decorated filaments. 2 days in vitro. Bar = 0.5 μm.

tents into a myotube is rather slow (26).

These subsarcolemmal cytoskeletal networks consisted mainly of 10-13 nm filaments. After treatment with S-1, most of these filaments were thickened and looked studded (decorated) along their length with numerous globular structures (Fig. 7). This decorated appearance confirmed that they are actin-containing filaments. Bundles of thin filaments were thought to be stress fibers. Filaments of 15-18 nm in diameter within this network were regarded as intermediate filaments. Short filaments of less than 8 nm in diameter were seen to cross-connect the lateral surfaces of other filaments to each other. From the surface of the network thick processes measuring about 100 nm in diameter extended (Fig. 3b). They appeared to be demembraned microvilli. More studies are required to confirm our present filament type diagnosis and, further, to identify other cytoskeletal structures, some of which may be hidden under the coated metal. To solve these problems, immunocytochemical procedures in combination with reduced metal coating but high resolution are required.

The present study has shown that the subsarcolemmal cytoskeletal network is not well formed in fusion-competent myoblasts, i.e., in cells at the period when they exhibit great lipid fluidity in their cell membranes (3), but is well developed in mature myotubes. Thus, although this structure contained many actin filaments, it seems to represent the membrane skeleton with a function of preserving the cell shape rather than being related to membrane mobility (13, 14, 28).

Myofibrillogenesis

Because of the presence of the cell membranes and intracellular amorphous substances, structures such as myofibrils, endoplasmic cytoskeletons and nuclei could not be seen by SEM via the usual sample preparation. These structures can be exposed for observation with SEM by the use of Triton, which solubilizes the membranes of the cell and extracts the bulk of the cytoplasm, leaving a residue composed of the elaborate systems of filaments and the nuclei. We have observed by SEM overall views of myofibrils in developing skeletal muscle cells *in vitro* with the osmium impregnation technique, using TCH as a ligand, after detergent extraction. This procedure permitted us to recognize developing myofibrils within the mass of cytoskeletons (12).

Within early myotubes at 2 days *in vitro*, thin bundles of filaments could be recognized (Fig. 8a). These bundles of filaments increased in number, girth and length, and at 7 days, they exhibited cross-striations (Fig. 8b), which were similar in appearance to those seen in adult myofibrils. Therefore, although cross-striations were not clearly discernible within thin bundles of filaments found in early myotubes, they seemed to correspond to myofibrils at the initial phase of their formation, as previously reported with TEM (29, 30). However, some of these filament bundles without cross-striations may represent stress fibers. It has been suggested that myofibril assembly seems to occur on, or in close association with, preexisting stress fibers (4). Thus, the direction of these filament bundles can generally be regarded as the same as that of myofibrillogenesis.

The pattern of distribution of myofibrils was generally correlated with the shape of the cells. In general, myofibrils were aligned close to, and parallel to the long axis of the cell within the straight part of the myotubes. At branching points of the myotubes most of the myofibrils ran along their lateral sides. Some myofibrils running along the inner sides of these branches were curved and split fan-wise (Fig. 8b). In flattened polygonal areas, myofibrils were prominent along the perimeters but some were also observed spanning the cellular diagonals (Fig. 8a).

It has been believed that stress influences the pattern of fibrillar structures in muscle cells (2, 17, 31). In this study, within straight portions of the myotubes, stress, which is caused by cell elongation and attachment to the substrate, will be oriented parallel to the longitudinal axis of the cell. The tension forces at branching points of the fused myotubes can be divided into components. We observed that the orientation of the myofibrils is similar to the inferred direction of tensional forces. In the polygonal area of the myotube, some of the inferred stress components run along the diagonals, and here also, myofibrils were found to run in such diagonal directions. This similarity suggests that a relationship between mechanical stress and myofibrillar alignment exists in cultured skeletal muscle cells. We propose that the relationship between stress and myofibrillar alignment is an obligatory one, and that it may in fact play an integral role in the response of cells to their physical environment. Further studies are required to clarify what factors establish the eventual orientation of the myotubes, and when and how stress orients the microfilaments.

Intracellular Membranous Organelles

Using the freeze-polishing or abrading method originally developed by Inoué and Osatake (11), we have observed the intracellular membranous structures of cultured muscle cells. In order to expose these structures, the osmium maceration technique (10) was additionally used to remove myofibrillar and other cytoskeletal structures. Generally, the membranous organelles could more properly be appreciated by SEM than by two-dimensional ultrathin sections.

By comparison with the thin section electron micrographs (6), we have tentatively identified the following structures. Mitochondria usually were long rod-shaped with complex irregular branchings, which could not be readily revealed by TEM. The T system was tubular in appearance with many warts, and it followed a tortuous course. Many of the sarcoplasmic reticulum appeared to be continuous with each other and often exhibited swellings (Figs. 9a, b). At such early stages of development, these two functionally related organelles were not yet arranged regularly (6), and thus, their distinction was sometimes difficult at low magnification. It should be feasible to distinguish the former

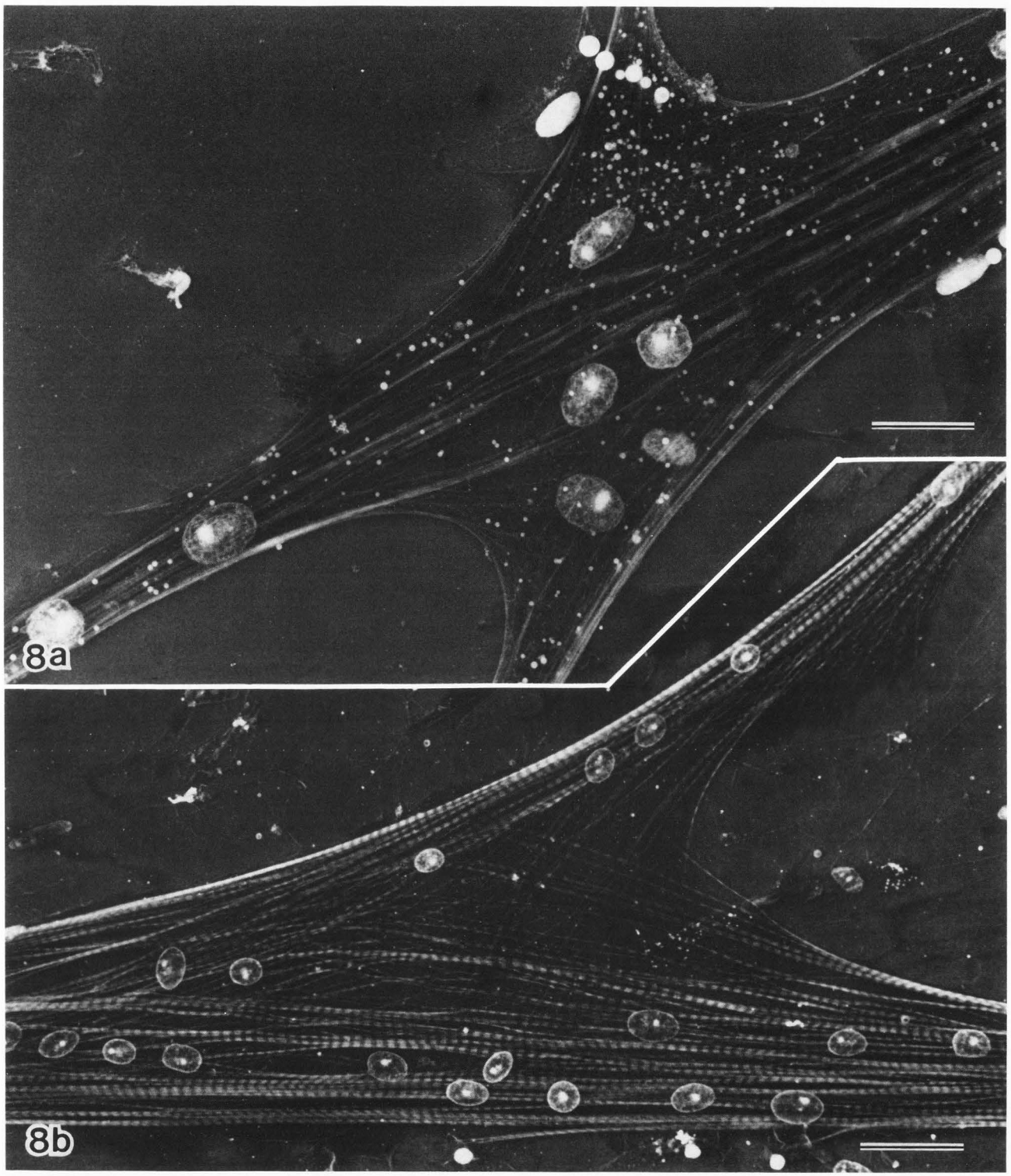

Fig. 8. Myofibrils are visualized by extraction of cells with Triton and subsequent staining with TCH-OsO_4. Myofibrils appear to run along the inferred direction of tension forces formed within cells. (a) 2 days in vitro. Bar = 10 μm; (b) 7 days in vitro. Bar = 20 μm.

structure from the latter by combining the impregnation of T system tubules with Golgi stain (25) with observation by back scattering electron imaging.

Conclusions

SEM has provided us with a unique opportunity to observe three-dimensionally the fine structure of the outer cell surfaces as well as various internal organelles of myogenic cells in culture. The results are of sufficient promise to encourage us to carry out more extensive analysis of myogenesis by SEM. With further progress in specimen preparation methods including immunocytochemistry, as well as the scanning electron microscope itself, and by combining these methods with appropriate observation modes of scanning electron microscopes (high resolution secondary emission, back scattering, scanning transmission, microanalysis, etc.), we will be able to obtain additional valuable information for understanding myogenic cell differentiation.

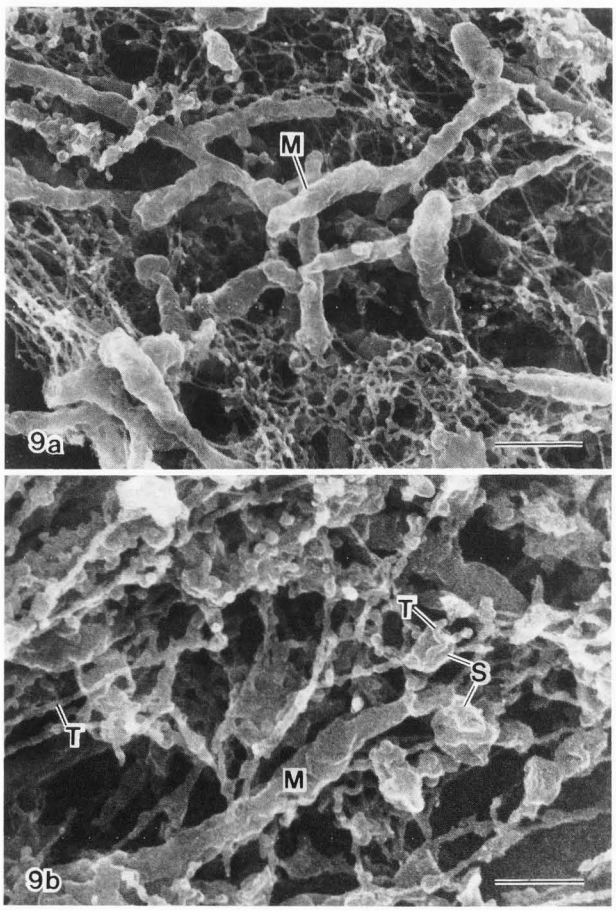

Fig. 9. Intracellular membranous organelles are visualized by freeze-polishing and osmium-maceration. Mitochondria, M; sarcoplasmic reticulum, S; T system tubules, T. (a) Bar = 1 μm, (b) 0.5 μm.

Acknowledgements

This research was supported by grants from the following: the Japanese Ministry of Education, Science and Culture; the Japanese Ministry of Health and Welfare (the National Center for Nervous, Mental and Muscular Disorders (NCNMMD 86-01-12) and for Cardiovascular Diseases); the Muscular Dystrophy Association of America. The authors wish to thank Dr. N. Toyota, Mrs. K. Shimizu and Mr. N. Nakamura for their technical assistance.

References

1 Buckley PA, Konigsberg IR. (1974) Myogenic fusion and duration of the post-mitotic gap (G_1). Dev Biol 37, 193-212.
2 Carey EJ. (1920) Studies in the dynamics of histogenesis. I. Tension of differential growth as a stimulus to myogenesis. J Gen Physiol 2, 357-372.
3 Connolly JA. (1984) Role of the cytoskeleton in the formation, stabilization, and removal of acetylcholine receptor clusters in cultured muscle cells. J Cell Biol 99, 148-154.
4 Dlugocz, AA, Antin, PB, Nachmias, VT, Holtzer, H. (1984) The relationship between stress fiber-like structures and nascent myofibrils in cultured cardiac myocytes. J Cell Biol 99, 2268-2278.
5 Erickson CA, Trinkaus JP. (1976) Microvilli and blebs as sources of reserve surface membrane during cell spreading. Exp Cell Res 99, 375-384.
6 Ezerman EB, Ishikawa H. (1967) Differentiation of the sarcoplasmic reticulum and T system in developing chick skeletal muscle in vitro. J Cell Biol 35, 405-420.
7 Fischman DA. (1972) Development of striated muscle. In: The Structure and Function of Muscle, Bourne GH (ed), 2nd ed, Academic Press, NY, vol 1, 75-149.
8 Fischman DA. (1986) Myofibrillogenesis and the morphogenesis of skeletal muscle. In: Myology, Engel AG, Banker BQ (eds), McGraw-Hill, NY, 5-37.
9 Galavazi G, Shenk H, Bootsma D. (1966) Synchronization of mammalian cells in vitro by inhibition of the DNA synthesis. Exp Cell Res 41, 428-437.
10 Inoué T. (1985) High resolution scanning electron microscopic cytology. Specimen preparation and intracellular structures observed by scanning electron microscopy. In: Science of Biological Specimen Preparation, Müller M, Becker R, Boyde A, Wolosewick JJ (eds), SEM Inc, AMF O'Hare, IL 60666, 245-256.
11 Inoué T, Osatake H. (1984) A freeze-polishing method for observing intracellular structures by scanning electron microscopy. J Electron Microsc 33, 356-362.
12 Isobe Y, Shimada Y. (1983) Myofibrillogenesis in vitro as seen with the scanning electron microscope. Cell Tissue Res 231, 481-494.

13 Isobe Y, Shimada Y. (1986) Organization of filaments underneath the plasma membrane of developing chicken skeletal muscle cells in vitro revealed by the freeze-dry and rotary replica method. Cell Tissue Res 244, 47-56.
14 Isobe Y, Shimada Y. (1986) Cytoskeleton of embryonic skeletal muscle cells. BioEssays 4, 167-171.
15 Isobe Y, Shimada Y, Manasek FJ. (1984) Cytoskeletons and myofibrils in cardiac myocytes in vitro observed by scanning and transmission electron microscopy. In: Congenital Heart Disease: Causes and Processes, Nora JJ, Takao A (eds), Futura, Mount Kisco, NY, 145-156.
16 Kelly RO, Dekker RA, Bluemink JG. (1973) Ligand-mediated osmium binding: its application in coating biological specimens for scanning electron microscopy. J Ultrastruct Res 45, 254-258.
17 Kulikowski RR. (1981) Myofibrillogenesis in vitro: implication for early cardiac morphogenesis. In: Perspectives in Cardiovascular Research, Pexieder T (ed), Academic Press, NY, vol 5, 367-379.
18 Masuko S, Ishikawa Y. (1983) Changes in surface morphology of myogenic cells during the cell cycle, fusion and myotube formation. Dev Growth Differ 25, 65-73.
19 Masuko S, Shimada Y. (1975) Surface morphology of chick myoblasts in vitro during the cell cycle and fusion. 10th Int Cong Anat, Science Council of Japan, Tokyo, 330.
20 Okazaki K, Holtzer H. (1966) Myogenesis: fusion, myosin synthesis, and the mitotic cycle. Proc Nat Acad Sci USA 56, 1484-1490.
21 Peng HB, Wolosewick JJ, Cheng PC. (1981) The development of myofibrils in cultured muscle cells: a whole-mount and thin-section electron microscopic study. Dev Biol 88, 121-136.
22 Porter KR, Anderson K. (1977) The morphogenesis of myofibrils from the microtravecular lattice as observed in cultured myoblasts. In: Muscle Contraction: its Regulatory Mechanism, Ebashi S, Maruyama K, Endo M (eds), Japan Sci Soc Press, Tokyo/Springer, Berlin, 527-540.
23 Porter K, Prescott D, Frye J. (1973) Changes in surface morpholgy of Chinese hamster ovary cells during the cell cycle. J Cell Biol 57, 815-836.
24 Ris H. (1985) The cytoplasmic system in critical-point dried whole mounts and plastic-embedded sections. J Cell Biol 100, 1474-1487.
25 Scales DJ, Yasumura T. (1982) Stereoscopic views of a dystrophic sarcotubular system: selective enhancement by a modified Golgi stain. J Ultrastruct Res 78, 193-205.
26 Shimada Y. (1971) Electron microscope observations on the fusion of chick myoblasts in vitro. J Cell Biol 48, 128-142.
27 Shimada Y. (1972) Scanning electron microscopy of myogenesis in monolayer culture: a preliminary study. Dev Biol 29, 227-233.
28 Shimada Y, Isobe Y. (1986) Cytoskeletal organization in embryonic chick skeletal muscle cells in vitro revealed by the detergent-extraction, freeze-dry method. In: Molecular Biology of Muscle Development, Emerson C, Fischman DA, Nadal-Ginard B, Siddiqui MAQ (eds), Alan R Liss, NY, 725-739.
29 Shimada Y, Obinata T. (1977) Polarity of actin filaments at the initial stage of myofibril assembly in myogenic cells in vitro. J Cell Biol 72, 777-785.
30 Shimada Y, Fischman DA, Moscona AA. (1967) The fine structure of embryonic chick skeletal muscle cells differentiated in vitro. J Cell Biol 35, 445-453.
31 Thornell LE, Sjöström M, Andersson KE. (1976) The relationship between mechanical stress and myofibrillar organization in heart Purkinje fibers. J Mol Cell Card 8, 689-695.
32 Wimber DE, Quastler H. (1963) A ^{14}C- and ^{3}H-thymidine double labeling technique in the study of cell proliferation in Tradescantia root tips. Exp Cell Res 30, 8-22.
33 Yaffe D. (1968) Retention of differentiation potentialities during prolonged cultivation of myogenic cells. Proc Nat Acad Sci USA 61, 477-483.

Discussions with Reviewers

H.B. Peng: The structures in Figs. 2-6 labeled as stress fibers do not have a distinct filamentous characteristic. Also, the size of the cytoskeletal filaments in the micrographs is much larger than those measured in thin sections. Comments on these points will be helpful.
Authors: Stress fibers probably lost the filamentous appearance by metal coating and/or drying shrinkage. The size of individual filaments in SEM micrographs became thicker by metal coating (2-4 nm).

Y.L. Wang: Although the number of microvilli per daughter cell appears to be lower (Fig. 1e), the total number of microvilli on both daughter cells seems similar to that on the mother cell (Fig. 1c). Therefore, the decrease in microvilli may reflect simply the division of microvilli between two cells.
Authors: Mathematically, provided the number of microvilli remains the same during cell division and the surface area of a mother cell at prophase is the same as that of two daughter cells at telophase, then the density of microvilli per unit area should remain the same before and after mitosis. However, microvilli appeared to have reduced in density during this period. The observation that microvilli reduced in number as cells proceeded through the cell cycle was supported by the fact that cells at early G_1 had much fewer number of microvilli at their surface.

Y.L. Wang: Could the differences in cytoskeleton reflect different sensitivity of the cortical filaments to extraction at different stages?
Authors: It is possible, but Triton extraction did not appear to have altered significantly cytoskeletal architectures at the subsarcolemmal domain. We compared organization of filaments underneath the plasma membrane revealed by the present SEM method with that observed by the freeze-fracture and deep-etch replica method without Triton treatment (Reference 13).

J.A. Connolly: What is the significance of the increased ruffling and blebbing of the membrane as cells proceed through the cell cycle?
Authors: The functional significance of blebs and ruffles is not entirely understood. Although blebs dominated the cell surface between G_2 and early G_1 of muscle cells, they were much fewer than those in other cell types. Nothing in our study suggests what they do and why they are formed. Erickson and Trinkaus (Reference 5) suggested blebs and microvilli as sources of reserve surface membrane during cell spreading. Ruffles became obvious on cells at G_1 and vanished during S and G_2. Since they were preferentially associated with the advancing edges of cells, they appear to be involved in cell locomotion as Abercombie et al. (Exp Cell Res 67, 359-367, 1971) has suggested.

J.A. Connolly: In mature myotubes, microtubules have been reported to twist helically around the myofibrils. Can you clearly identify which fibers are microtubules and if so, what is their relationship to developing myofibrils?
Authors: Microtubules have been found in the deep endoplasmic cytoskeletal domain by freeze-fracture deep-etch method (References 13, 14, 28). Since we observed the subsarcolemmal cytoskeletal domain in this study (Figs. 2-6), microtubules were not clearly visible. Further, in the cells treated with TCH-OsO_4 (Fig. 7), the resolution was not enough to see microtubules.